



OPEN

Screening of cashmere fineness-related genes and their ceRNA network construction in cashmere goats

Taiyu Hui, Yuanyuan Zheng, Chang Yue, Yanru Wang, Zhixian Bai, Jiaming Sun, Weidong Cai, Xinjiang Zhang, Wenlin Bai & Zeying Wang✉

Competitive endogenous RNA (ceRNA) is a transcript that can be mutually regulated at the post-transcriptional level by competing shared miRNAs. The ceRNA network connects the function of protein-encoded mRNA with the function of non-coding RNA, such as microRNA (miRNA), long non-coding RNA (lncRNA), and circular RNA (circRNA). However, compared with the ceRNA, the identification and combined analysis of lncRNAs, mRNAs, miRNAs, and circRNAs in the cashmere fineness have not been completed. Using RNA-seq technology, we first identified the miRNAs presented in Liaoning Cashmere Goat (LCG) skin, and then analyzed the mRNAs, lncRNAs, circRNAs expressed in LCG and Inner Mongolia cashmere goat (MCG) skin. As a result, 464 known and 45 new miRNAs were identified in LCG skin. In LCG and MCG skin, 1222 differentially expressed mRNAs were identified, 170 differentially expressed lncRNAs and 32 differentially expressed circRNAs were obtained. Then, qRT-PCR was used to confirm further the representative lncRNAs, mRNAs, circRNAs and miRNAs. In addition, miRanda predicted the relationships of ceRNA regulatory network among lncRNAs, circRNAs, miRNAs and mRNAs, the potential regulatory effects were investigated by Go and KEGG analysis. Through the screening and analysis of the results, the ceRNA network regulating cashmere fineness was constructed. lncRNA MSTRG14109.1 and circRNA452 were competed with miRNA-2330 to regulated the expression of TCHH, KRT35 and JUNB, which may provide a potential basis for further research on the process of regulating the cashmere fineness.

Liaoning Cashmere Goat is a goat breed with high-quality cashmere in China which originated in southeastern Liaoning Province. The variety has an advantage in producing cashmere and ranks first in the country. The cashmere goats of Inner Mongolia are mainly distributed in the northwest of Inner Mongolia Plateau, and their diameter is smaller than that of LCG, which takes advantage of this breed¹. Wool collected from cashmere goats can be made into cashmere and clothing resisted the cold, which is in tremendous demand in the international market². Later it was found that cashmere fineness was the main factor in the quality of cashmere. So far, the specific regulatory mechanism of cashmere fineness is not well realized. In order to explore further the key mechanism affecting cashmere fineness in cashmere goat skin. We studied and analyzed in two different types of cashmere fibers, searched for the key genes regulating cashmere fineness and the molecular mechanism regulating cashmere fineness expression. MiRNA is a type of non-coding RNA with a length of about 22 nt. It plays a key role in post-transcriptional gene regulation, and its goal is to target mRNAs to translational suppression and gene expression as an adaptor of the miRNA-induced silencing complex³. A single miRNA can simultaneously targets multiple target genes and influences the expression of signaling pathways involved in functional expression⁴. In the past, some miRNAs have been found in the skin of goats⁵. Some studies have found that miRNA interacts with target genes and lncRNA affects cashmere growth.

lncRNA is different classes of RNA molecules that are longer than 200 nucleotides⁶. Recent studies have shown that lncRNA regulates different levels of genes and has developmental and differentiation functions for organisms⁷. lncRNA can interacts with mRNA, miRNA and can arouset a number of different functions⁸. For example, lncRNA XLOC_008679 is involved in the regulation of cashmere fineness by targeting *KRT35*⁹.

College of Animal Science & Veterinary Medicine, Shenyang Agricultural University, Shenyang 110866, China.
✉email: wangzeying2012@syau.edu.cn

Sample	Raw reads	Valid reads	Q20%	Q30%	GC content%
LCG	136,441,946	128,989,956	98.72	89.48	50
MCG	154,106,016	146,038,848	99.01	91.89	46

Table 1. Sequence statistics and quality control of lncRNAs, circRNAs and mRNAs.

Furthermore, lncRNA MTC promotes fibroblast proliferation and regulates cashmere growth by activating NF- κ B signaling pathway¹⁰.

Circular RNAs (circRNAs) are a novel type of long, non-coding RNAs¹¹. It is a closed continuous loop distinct from linear RNA¹². Studies suggest that circRNA may be involved in mammalian growth and differentiation and cancer¹³. In the past, few studies have shown that circRNA regulates the fineness of cashmere, nowadays, there is new evidence that circRNA may regulate the growth of cashmere¹⁴.

The molecular mechanism of ceRNA on regulating the growth and fineness of cashmere is unclear. Therefore, in order to understand the effect of ceRNA network on cashmere fineness, this study focus on the differential expression patterns of lncRNA, mRNA, and circRNA in the skin via high-throughput sequencing. Differentially expressed circRNAs, lncRNAs, and mRNAs were further confirmed using qRT-PCR. Subsequently, we constructed lncRNA-miRNA-mRNA, circRNA-miRNA-mRNA, lncRNA/circRNA-miRNA-mRNA ceRNA network in the skin of cashmere goats based on the interaction of lncRNA-miRNA, circRNA-miRNA and mRNA-miRNA. Our findings might provide new evidence for exploring the cashmere fineness regulation mechanism.

Results

Differential expression of lncRNAs, circRNAs, mRNAs and miRNAs. After the samples were extracted from the total RNA library for high throughput sequencing, we got 136,441,946 and 154,106,016 raw reads (Table 1). 128,989,956 and 146,038,848 valid data were obtained after removing adaptors and low-quality sequencing data. The screening conditions are $q\text{-value} \leq 0.05$ and $|\log_2\text{FoldChange}| \geq 1$, it was found that a total of 1222 mRNAs were differentially expressed between the two groups of samples, including 187 up-regulated in LCG and 1035 down-regulated in LCG (Figs. 1, 2B).

170 lncRNAs were differentially expressed between the two groups of samples (Fig. 1A), including 67 up-regulating lncRNAs and 103 down-regulating in LCG (Fig. 2A). In up-regulation, MSTRG.5418.1, MSTRG.11385.1 showed slightly higher expression abundance and multiple than others, which may have important functions and are the main directions for follow-up studies.

A total of 32 circRNAs were differentially expressed (Fig. 1C), including 17 up-regulated in LCG and 15 down-regulated (Fig. 2C)¹⁴. Some genes can regulate multiple circRNAs, such as *TCHH*, which regulate four transcripts of ciRNA126, ciRNA127, ciRNA128, ciRNA129, through the analysis of differential expression of non-coding RNA. We collected skin samples and examined the expression of miRNA and small RNA in LCG (Fig. 1D). The sequencing results obtained an total of 15,245,657 raw reads (Table 2)¹⁵. Li et al. sequenced the miRNAs in the skin of MCG by high throughput¹⁶. After compared our data with theirs, 147 miRNAs with different expression were obtained, including 69 up-regulated miRNAs and 78 down-regulated miRNAs ($q\text{-value} \leq 0.05$ and $|\log_2\text{twofold change}| \geq 1$) (Fig. 2D).

Differentially expressed lncRNAs/circRNAs/mRNAs/miRNAs validated by qRT-PCR. To verify the results of the RNA-seq, we randomly selected 14 circRNAs, 24 lncRNAs, 24 miRNAs and 7 mRNAs in fine type LCG (FT-LCG) and coarse type LCG (CT-LCG) panels for qRT-PCR verification. The high-throughput results showed the difference between the diameters of the fine and the coarse types (Fig. 3). According to the $2^{-(\Delta\Delta Ct)}$ numerical values, it can be seen that the trend between the qRT-PCR results and the results of RNA-seq was consistent (Fig. 4). The expression level of FT-LCG is higher than that of CT-LCG, which may play a positive role in regulating candidate genes related to cashmere fineness. However, the expression level of CT-LCG is higher than that of FT-LCG, which may negatively regulate candidate genes related to cashmere fineness.

Analysis between lncRNAs, circRNAs, miRNAs and mRNAs differential expression. We mainly performed predictive analysis of differential expression mRNAs, lncRNAs, miRNAs and circRNAs in RNA-seq results. By analyzing circRNA-mRNA, the results yield a key host gene, *TCHH*, which is simultaneously up-regulated in mRNA and circRNA. The 30 lncRNA-mRNA were significantly different, including 6 up-regulated mRNAs, 16 down-regulated mRNAs, 2 lncRNA target genes up-regulated, and 5 lncRNA target genes down-regulated. It was found that some key differentially expressed miRNAs can regulate related genes, such as miRNA-660-*KRT26*, miRNA-199a-3p-*DSG4*. MiRNA-125b, miRNA-19a (b), miRNA-339b, which may play a regulatory role in the target gene *KRT35*. MiRNA-141, miRNA-1940, miRNA-200a, miRNA-7 may be involved in the regulation of the target gene *JUNB*. Joint analysis found that the up-regulated mRNA *LOC108634775/XM_018045014.1* was both a target gene for up-regulated lncRNAs and a target gene for down-regulated lncRNAs (Fig. 5). Suggesting that a large number of genes may be regulated from different lncRNAs transcripts, whose expression are performed under the combined action of individual transcripts. Some of these genes are neither the up-regulated lncRNAs target gene nor the down-regulated lncRNAs target gene, indicating that this part of the gene expression may not be regulated by the relevant lncRNAs.

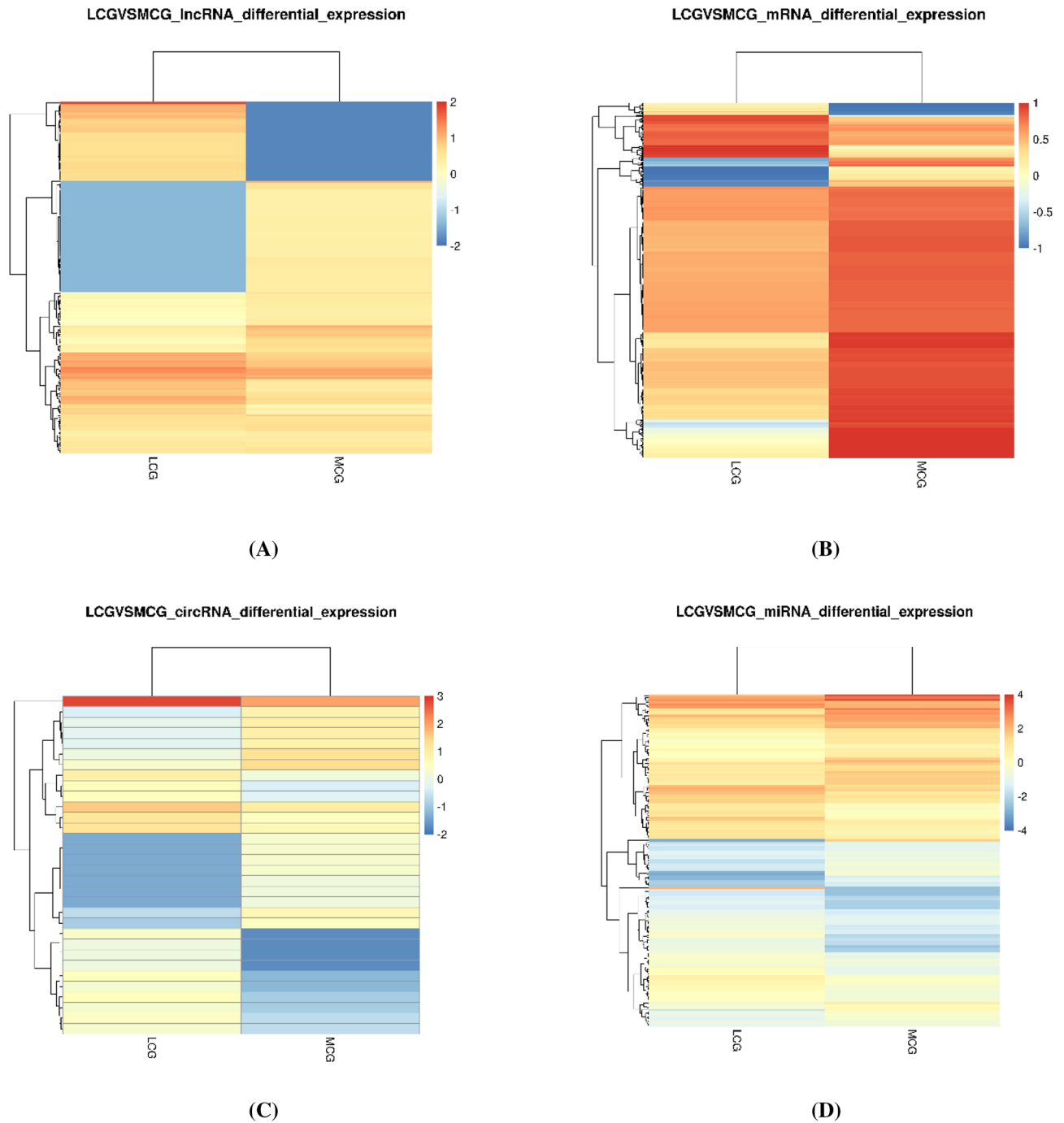


Figure 1. Heatmap of DElncRNAs, mRNAs, circRNAs and miRNAs between LCG and MCG. (A) Heatmap of DElncRNAs. (B) Heatmap of DEMRNAs. (C) Heatmap of DEcircRNAs. (D) Heatmap of DEmiRNAs.

Prediction of LncRNA–miRNA interactions. LncRNAs contain specific binding sequences of miRNAs, which can reduce their levels in the cytoplasm by adsorbing miRNAs to relieve the inhibition effect of miRNAs on target gene expression. In this section, the miRanda program was used to predict the targeted regulatory relationship between lncRNAs and miRNAs (Table 3). The results found that 458 interacted with miRNA–lncRNA.

Prediction of circRNA–miRNA interactions. CircRNA can be used as an endogenous competing RNA by adsorbing miRNAs and some undiscovered ways to release the inhibition of miRNAs on their target genes, up-regulate the expression of target genes and then participate in the regulation of gene expression. The miRNAs and circRNAs were jointly analyzed by miRanda, resulting in 153 miRNA–circRNA relationship pairs, and finally 41 relationship pairs were screened out by the critical points predicted by software (Table 4).

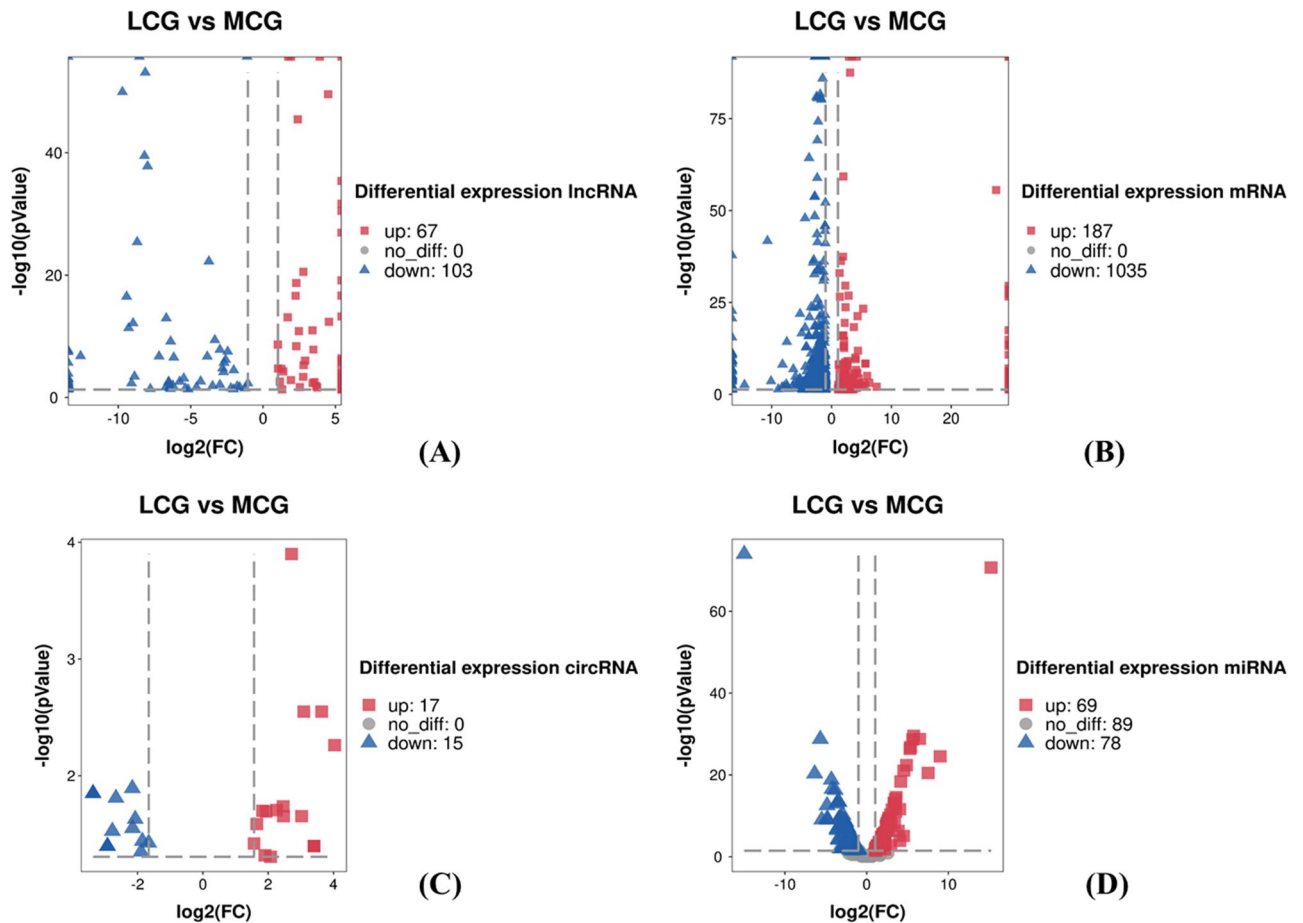


Figure 2. Volcano plot of DElncRNAs, mRNAs, circRNAs and miRNAs between LCG and MCG. (A) Volcano plot of DElncRNAs. (B) Volcano plot of DEmRNAs. (C) Volcano plot of DEcircRNAs. (D) Volcano plot of DEmiRNAs.

Prediction of miRNA–mRNA interactions. MiRNAs can combine the target sequences of the untranslated ends of mRNAs to silence the mRNAs after transcription. The main mechanisms include promoting the degradation of mRNAs and inhibiting the translation of mRNAs. In order to better understand their potential functions, miRanda was used to analyze the targeted mRNAs of miRNAs. A total of 17,301 miRNA–mRNA relationship pairs were obtained, and 5605 relationship pairs were finally obtained through conditional screening (Table 5).

Sample	Reads	Bases	Error rate (%)	Q20 (%)	Q30 (%)	GC content (%)
LCG	15,245,657	0.762G	0.01	97.98	93.08	49.24

Table 2. Sequence statistics and quality control of miRNAs.

GO and KEGG pathway analyses of differentially-expressed mRNAs. In the previous results, we predicted the target mRNA of miRNA based on miRanda, these target mRNAs are now compared with the differentially expressed mRNAs identified in the RNA-seq results to obtain 1062 differentially expressed mRNAs, of which 160 are up-regulated. To further understand the functional role of 160 differentially expressed mRNAs (DEmRNAs) in cashmere fineness, we use DIVAD to analysis of GO and KEGG functional enrichment (Fig. 6). Based on the condition of $p < 0.05$, GO analysis is mainly significantly enriched in intermediate filament (CC) and structural molecule activity (MF) terms. The eight pathways enriched are shown as table, which may be key pathways to regulate the growth of cashmere fibers (Table 6).

Construction of lncRNA/circRNA–miRNA–mRNA network. In this part, we selected 44,771 lncRNA–miRNA–mRNA interaction pairs. Considering that the total interaction network is too complex, it only demonstrates the expression regulation relationship with 160 up-regulated mRNAs as the core genes, which yielded 3060 lncRNA–miRNA–mRNA relation pairs, including 103 up-regulated mRNAs combined with 61 miRNAs

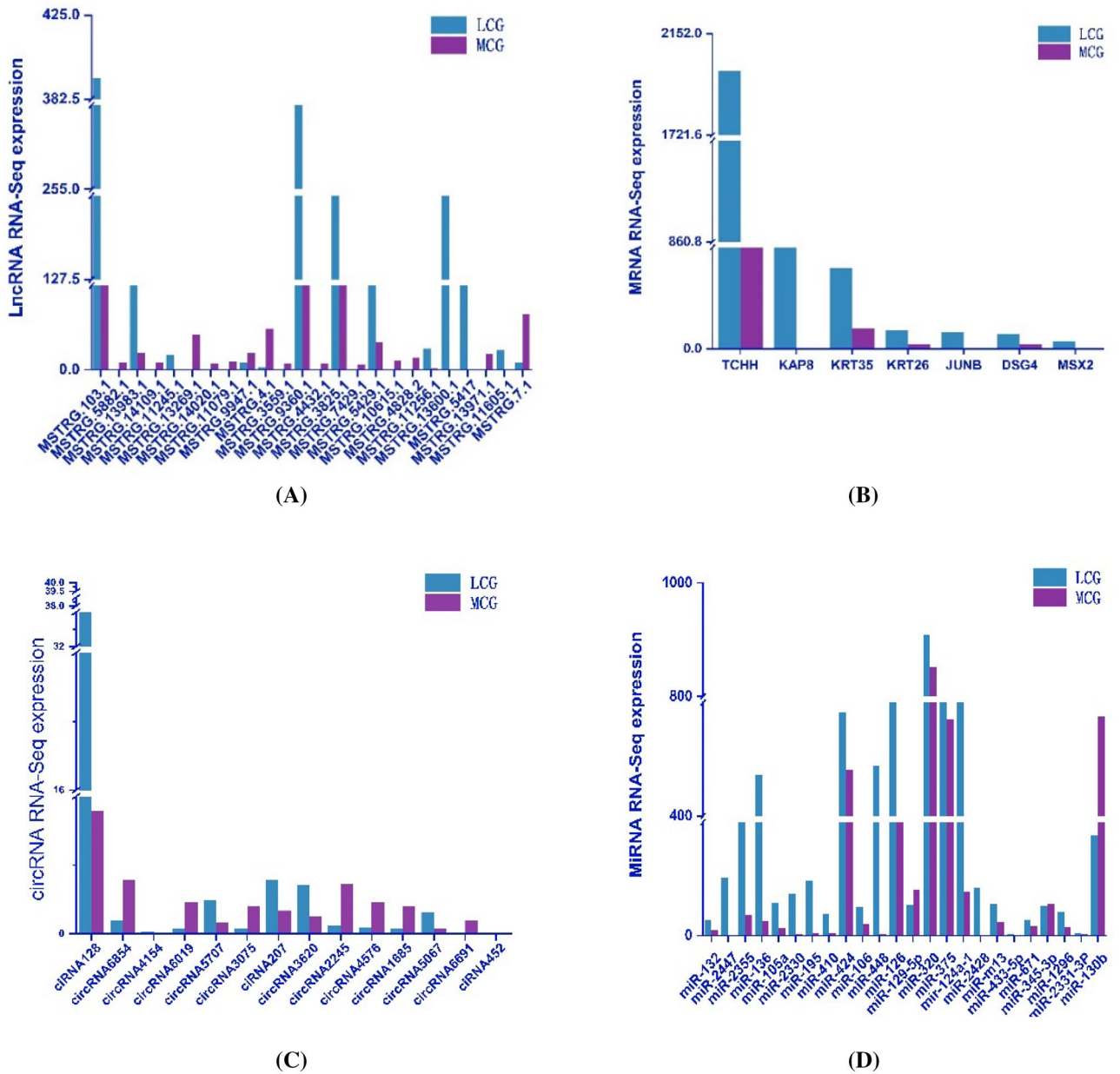


Figure 3. DElncRNAs, mRNAs, circRNAs and miRNAs between LCG and MCG in RNA sequencing (RNA-seq). **(A)** DElncRNAs between LCG and MCG in RNA-seq. **(B)** DEmRNAs between LCG and MCG in RNA-seq. **(C)** DEcircRNAs between LCG and MCG in RNA-seq. **(D)** DEMiRNAs between LCG and MCG in RNA-seq.

and 195 lncRNAs. Construct a network regulation relationship of lncRNA–miRNA–mRNA with lncRNAs as decoy, miRNAs as core and mRNAs as target. Some key ceRNA networks were derived from the graph (Fig. 7), MSTRG.11079.1–miR-106–*DSG4*; MSTRG.4.1–miR-126–*TCHH*; MSTRG.14109.1 and miR-2330 co-regulate *JUNB*, *MSX2*, *KRT35* and *TCHH*.

According to the theory of ceRNA and existing research, we find circRNA–mRNA interaction pairs with the same miRNAs binding site, and construct circRNA–miRNA–mRNA interaction pairs with circRNAs as decoy, miRNAs as core and mRNAs as targets. The predicted results showed that there were 4497 circRNA–miRNA–mRNA interaction pairs. Similarly, considering that all interaction networks are too complex, only 160 up-regulated mRNAs are shown as the core to bind the circRNAs and miRNAs, and 308 CircRNA–miRNA–mRNA relationship pairs are obtained, including 81 up-regulated mRNAs that bind to 32 miRNAs and 24 circRNAs (Fig. 8). The results showed that circ6854–miRNA-106–*DSG4*; circ3075–miRNA-129-5p–*TCHH*; circ452 and miRNA-2330 act simultaneously with *MSX2*, *TCHH*, *KRT35* and *JUNB*, which may be important regulatory pathways of cashmere fineness.

For a deeper understanding of the interactions between lncRNAs, miRNAs, mRNAs, and circRNAs. The network of regulation relationship of lncRNA/circRNA–miRNA–mRNA was constructed under the

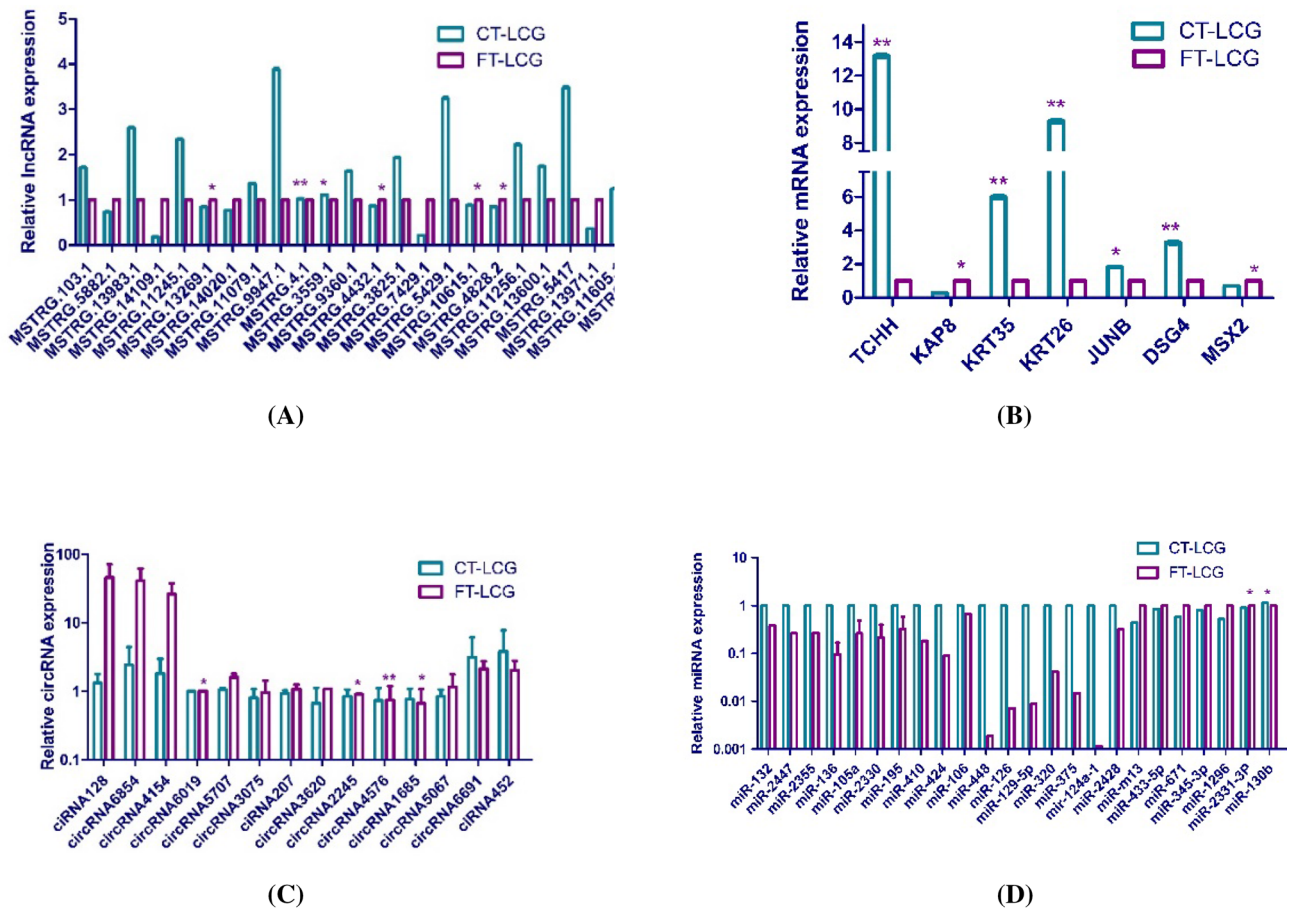


Figure 4. QRT-PCR verification of DElncRNAs, mRNAs, circRNAs and miRNAs between CT-LCG and FT-LCG. (A) DElncRNAs between CT-LCG and FT-LCG validated by qRT-PCR. (B) DEmRNAs between CT-LCG and FT-LCG validated by qRT-PCR. (C) DEcircRNAs between CT-LCG and FT-LCG validated by qRT-PCR. (D) DEmiRNAs between CT-LCG and FT-LCG validated by qRT-PCR.

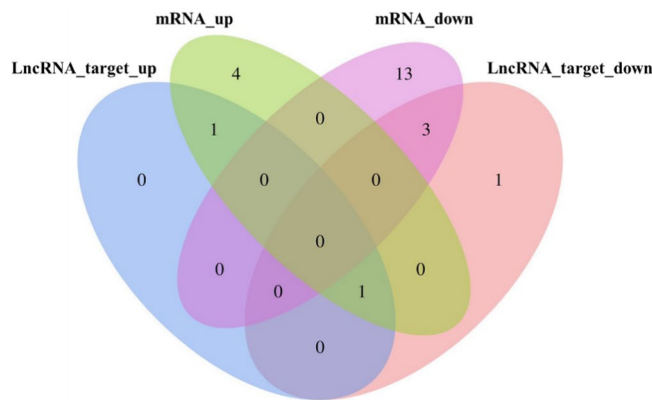


Figure 5. Venn gram showing the Integrative analysis of lncRNA targets and mRNAs.

interaction of lncRNA–miRNA, circRNA–miRNA and miRNA–mRNA (Fig. 9). The analysis shows that lncRNA-MSTRG.14020.1, lncRNA-MSTRG.11256.1, lncRNA-MSTRG.9947.1, lncRNA-MSTRG.13269.1, lncRNA-MSTRG.3736.1, lncRNA-MSTRG.10487.1 and circ6348 are ceRNA of miR-1224, and the target gene is *KAP8*. While lncRNA-MSTRG.706.1, lncRNA-MSTRG.9947.1, lncRNA-MSTRG.5882.1, lncRNA-MSTRG.13983.1, lncRNA-MSTRG.10487.1, lncRNA-MSTRG.11754.1, lncRNA-MSTRG.10615.1, and circ6691 are miR-105a targets ceRNA of *KRT26* (Fig. 10). Objective to construct the ceRNA regulatory network of non-coding RNA in cashmere goat skin and predict the network that may play a role in cashmere fineness growth.

lncRNA	miRNA	TargetScan_score	miRanda_Energy
MSTRG.11245.1	miR-185	96	-22.24
MSTRG.13925.1	miR-2476	97	-16.14
MSTRG.1626.1	miR-132	98	-12.33
MSTRG.18.1	miR-193a-5p	97	-21.61
MSTRG.3825.1	miR-320	97	-19.13
MSTRG.3829.1	miR-2428	97	-21.89
MSTRG.7654.1	miR-488	96	-14.60
MSTRG.7899.1	miR-339	96	-26.44
MSTRG.9911.1	miR-136	96	-17.01
MSTRG.12784.1	miR-2411	97	-16.74
MSTRG.4.1	miR-126	96	-11.28
MSTRG.3970.1	miR-2447	97	-29.56
MSTRG.10487.1	miR-9	96	-12.69
MSTRG.10615.1	miR-1343	96	-17.07
MSTRG.4383.1	miR-212	96	-12.67
MSTRG.4383.1	miR-545	96	-11.41

Table 3. Interaction versus between lncRNA–miRNA. Table shows that the num of TargetScan fractional percentiles ≥ 96 , $-30 <$ the num of Miranda maximum free energy values < -10 .

circRNA	miRNA	TargetScan_score	miRanda_Energy
ciRNA156	miR-2447	88	-46.11
circRNA1685	miR-375	80	-26.32
circRNA3620	miR-2331	80	-17.68
circRNA5707	miR-136	80	-18.74
circRNA6893	miR-9	80	-10.02
circRNA815	miR-195	80	-11.75
circRNA815	miR-424	80	-31.55

Table 4. Interaction versus between circRNA–miRNA. Table shows that the num of TargetScan fractional percentiles ≥ 80 , $-50 <$ the num of Miranda maximum free energy values < -10 .

mRNA	miRNA	TargetScan_score	miRanda_Energy
ACSL4	miR-375	99	-10.69
IQGAP2	miR-545	99	-10.04
LOC102179433	miR-2307	99	-10.21
MRC1	miR-488	99	-10.70
P2RY13	miR-375	99	-10.66
PLXDC2	miR-375	99	-10.48
SPATS2L	miR-105a	99	-10.92
TMSB4X	miR-448	99	-10.77

Table 5. Interaction versus between miRNA–mRNA. Table shows that the num of TargetScan fractional percentiles ≥ 99 , $-11 <$ the num of Miranda maximum free energy values < -10 .

Discussion

Non-coding RNAs (ncRNAs) make up most of the transcribed genome and play different roles in numerous cellular processes. ncRNA includes such as miRNA, circRNA, and lncRNA¹⁷. Many studies have shown that these ncRNAs participate in competitive regulatory interactions, which is ceRNA networks¹⁸. Recently, studies have confirmed the significance of ceRNA in the regulation of skin diseases¹⁹ and hair follicle circulation²⁰. The growth of cashmere is affected by many factors. The experimental samples are from modern standardized large-scale farms. With the same feeding standards and feeding environment, we want to analyze the differences in cashmere production from the genetic background. Based on the characteristics of LCG and MCG, we used

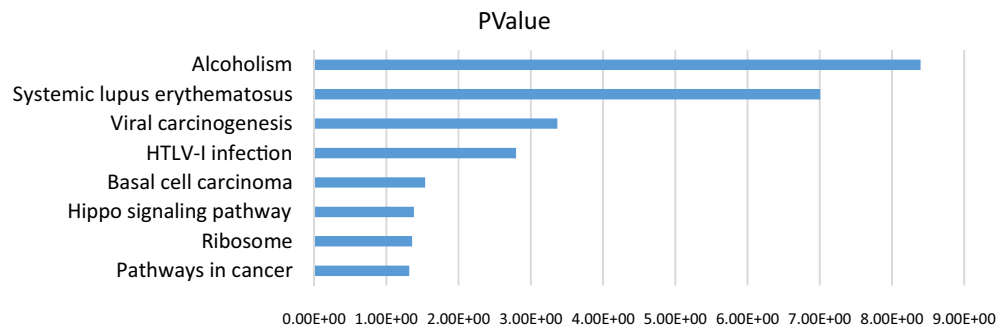


Figure 6. KEGG pathway analysis of 160 differentially expressed (DE) mRNAs.

Term	Pathway ID	Count	p value	Fold enrichment
Alcoholism	chx05034	11	4.02E-09	13.20952698
Systemic lupus erythematosus	chx05322	9	9.86E-08	14.5951417
Viral carcinogenesis	chx05203	7	4.30E-04	6.776315789
HTLV-I infection	chx05166	7	0.001605	5.270467836
Basal cell carcinoma	chx05217	3	0.028931	10.94635628
Hippo signaling pathway	chx04390	4	0.041647	5.026141513
Ribosome	chx03010	5	0.043986	3.620932101
Pathways in cancer	chx05200	6	0.048187	2.904135338

Table 6. KEGG pathway analysis of 160 DE mRNAs.

these two breeds as high-throughput sequencing samples and constructs the regulatory relationship structure of the ceRNA network based on the correlation between ncRNAs. The difference of sequencing results indicated the difference of genetic material in different varieties. No research has been reported on the regulation of the ceRNA network related to LCG cashmere fiber growth thus far. Therefore, we first constructed a ceRNA regulatory network in cashmere goat skin.

We obtained maps of lncRNAs, circRNAs, mRNAs and miRNAs expression by high-throughput sequencing. The qRT-PCR results are basically consistent with the results of high-throughput analysis. In recent decades, the role of many genes in the regulation of cashmere goat growth has been widely studied. In recent years, researchers have reported that some genes can regulate cashmere fiber diameter through targeting relationships, such as *KRT6A*, *KRT38*, *KRT26*, *KRT32*, *KRT82*, *EGR3*, *FZD6*, *LncRNAMTC*, *KAP6.2*, *KAP7.1*, *KAP11.1*, *K26*, *BMPR_IB*, *LAMTOR3*, *KAP8.2* and *KAP26.1*, etc.^{10,21,22}. In our study, 160 differentially expressed mRNAs were found by comparison. Among them, *MSX2*²³, *KRT26*, *KRT35* and *KAP8*²⁴ have been reported to affect cashmere growth and cashmere fineness in cashmere goats. *TCHH*^{22,25}, *DSG4* expression in sheep skin²⁶. *JUNB* can regulate epidermal stem cells and sebaceous glands by balancing the proliferation and differentiation of progenitor cells and suppressing lineage infidelity²⁷. In mice, lack of *JUNB* wounds in skin delays healing and epidermal hyper proliferation²⁸ and differential expression in the mammary glands of suckling goats²⁹. However, most genes are regulated at the transcriptional level. Therefore, we speculated that these genes may have some role in regulating cashmere growth.

In order to further explore the key factors affecting the regulation of cashmere growth, we used miRanda and TargetScan to predict the relationship between lncRNA-miRNA, circRNA-miRNA, miRNA-mRNA. MiRNA, by pairing with bases of complementary sequences in mRNA molecules, can induce gene silencing by binding incomplete complementarity to mRNA 3'-non-translational regions (3'-UTRs)^{30,31}. MiRNAs play an important role in gene regulation in plants and animals³². It has been reported that miRNA-mRNA interactions may affect cashmere growth. For example, the genes associated with cashmere growth in the Wnt signaling pathway are *FZD6*, *LEF1*, *FZD3*, *WNT5A*, and *TCF7*, and related miRNAs are miR-195, miR-148a, miR-4206, and recently, several groups have reported that gene products can regulate miRNA activity, and different RNA abundance values alter ceRNA interactions³³.

LncRNA has multiple functions, including transcriptional activation, silencing of protein-coding genes, and interaction with mRNA or miRNA to regulate its function. Studies indicate that lncRNA-HOTAIR transcripts may be related to the formation and growth of cashmere fiber³⁴. In recent years, lncRNA has become a previously undiscovered gene expression regulator that can regulate various cellular processes. Related research reports lncRNA LNC_000972, LNC_000503 and LNC_000881 may regulate hair follicle circulation through genes of *WNT3A*, *HOXC13* and *MSX2*³⁵. Increasing evidence suggests that the effect of lncRNA on mRNA may regulate its function. Studies have found that the relative expression of *ET-1*, *SCF*, *ALP* and *LEF1* in dermal papilla cells can be increased by increasing the expression of lncRNA-000133, which may be related to the formation and

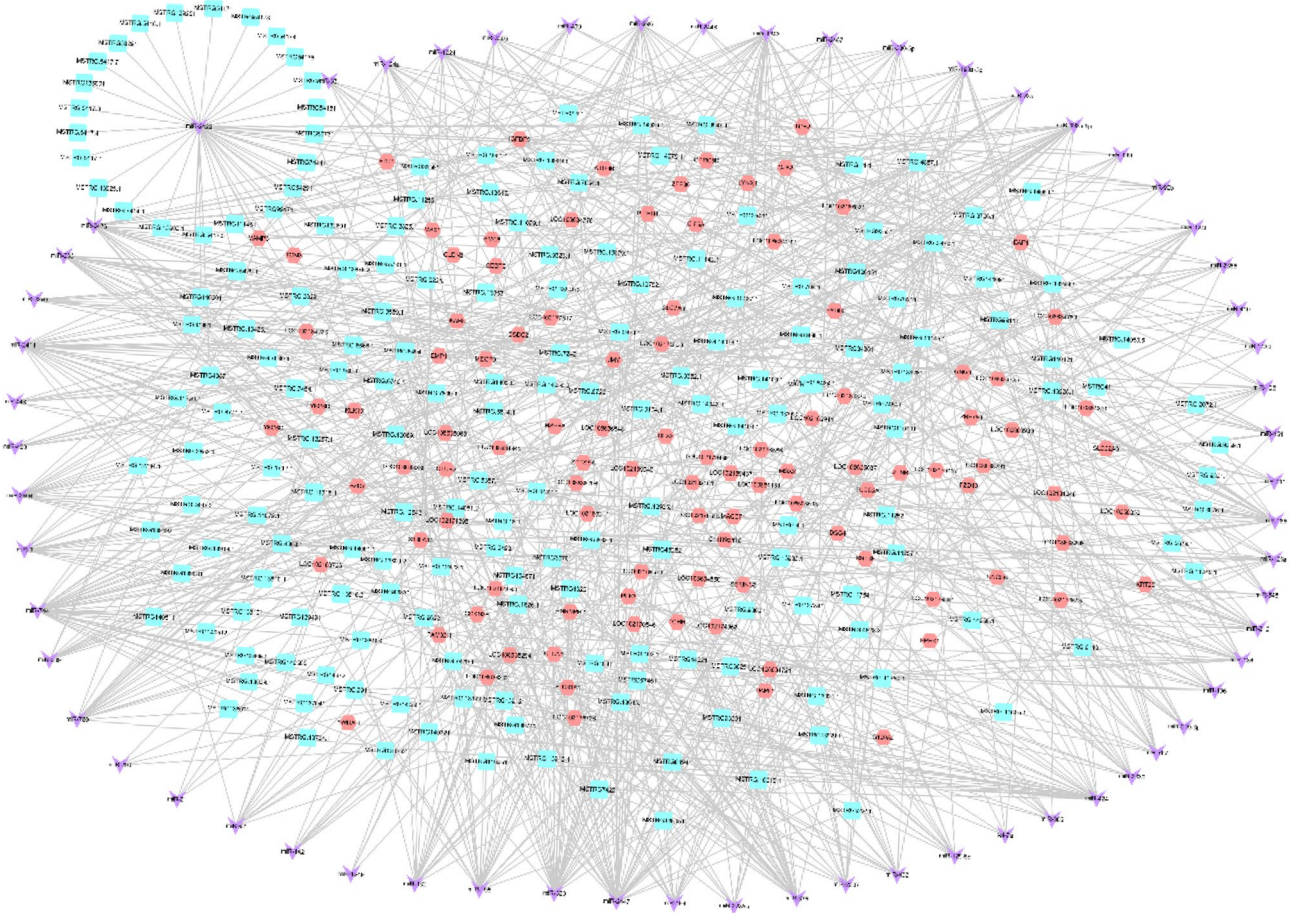


Figure 7. Regulation network of lncRNA–miRNA–mRNA. Pink: mRNAs, blue: lncRNAs, purple: miRNAs.

growth of cashmere fibers³⁶. Later research found that lncRNA can affect cashmere growth through mutual regulation with target genes³⁷.

The covalently enclosed circRNA is produced by back-splicing the precursors of the exons of thousands of genes in eukaryotes³⁸, which makes the resistance to nucleic acid exonuclease enhanced and therefore stable³⁹. Emerging evidence suggests that circRNA a key role in cancer⁴⁰, cell growth and differentiation⁴¹. In the Steroid-induced osteonecrosis of the femoral head-bone marrow mesenchymal stem cells, five circRNA targeted mRNAs including *CLASP1*, *ENOX2*, *SYK*, *UBE2G2*, and *WNT5B* were up-regulated by circRNA⁴². It has been proven in animals that it can be regulated by establishing a network of dynamic regulatory relationships between circRNA and mRNA⁴³. The three circRNAs (chi-circ-1926, chi-circ-2829, and chi-circ-0483) and their corresponding host genes (*BNC2*, *PAPPA*, and *ZNF638*) may have certain functional roles in the development of cashmere fiber growth by constituting perfect regulatory pairs⁴⁴.

Here, we build the lncRNA/circRNA–miRNA–mRNA ceRNA network based on our data for the first time. Nevertheless, the activity of some miRNAs has been shown to be mediated by lncRNA, further reducing the number of miRNA able to bind to mRNA target activity by separating the said activity⁴⁵. Research indicates that the lncRNA–miRNA–mRNA regulatory network may play a role in the growth of cashmere fibers. For instance, the putative lncRNA-599554 may regulate the expression of potential target genes by regulating the expression of four miRNAs (miR-548d-3p, miR-15a-5p, miR-497-5p and miR-424-5p), such as *AXIN2*, *BTRC*, *CCND1* and *WNT5A*, miR-17-5p target two putative lncRNAs: lncRNA-599618 and lncRNA-599556, which are also involved in the regulation of *MYC*, *CCND1*, *CCND2*, *MAPK9* and *SMAD4* genes³⁷. Then, the ceRNA network miR-221-5p-lnc_000679-*WNT3*, miR-34a-lnc_000181-*GATA3*, and miR-214-3p-lnc_000344-*SMAD3* have regulatory roles in hair follicle biology of cashmere goats³⁵. Therefore, it is clear that the lncRNA–miRNA–mRNA interaction ultimately regulates the expression pattern of the target gene.

In recent years, because circRNA contains miRNA response elements and competes with mRNA, the potential of circRNA as a gene regulator has shown⁴⁶. CircRNA inhibits the function of miRNA as a miRNA sponge through a competitive endogenous RNA (ceRNA) network, and then regulates mRNA expression through the intended target site of the miRNA⁴⁷. Some studies have identified a potential target for regulating receptive endometrium development by regulating the expression of circRNA-9119-miR-26a-*PTGS2* in endometrial epithelium cells⁴⁸. It was pointed out that circular RNA may play an important role in the secondary hair follicles of cashmere goats through the circRNA–miRNA–mRNA regulatory network, which explained the molecular mechanism of secondary hair follicle development and cashmere fiber growth in cashmere goats⁴⁴.

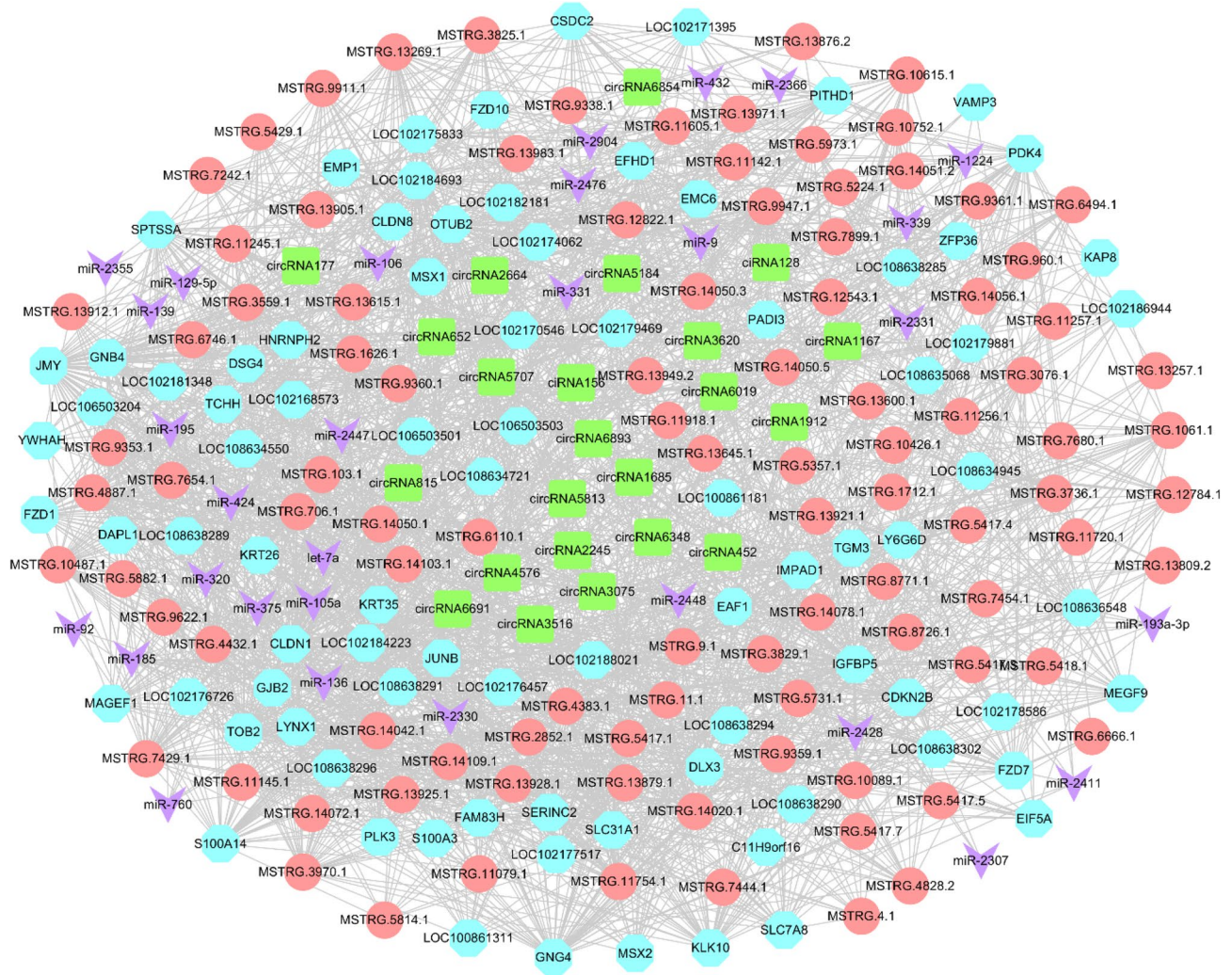


Figure 9. Regulation network of lncRNA/circRNA–miRNA–mRNA. Pink: lncRNAs, green: circRNAs, blue: mRNAs, purple: miRNAs.

Materials and methods

Ethics statement. All experimental protocols were approved by the Laboratory Animal Management Committee of Shenyang Agricultural University (No. 201806011, Shenyang, China). All methods were carried out in accordance with relevant guidelines and regulations. The study was carried out in compliance with the ARRIVE guidelines.

Sample processing. We collected each samples of three adult female Liaoning cashmere goat scapular skins of Animal Husbandry Science Liaoning Province and three adult female Inner Mongolia cashmere goat scapular skins of Inner Mongolia Hohhot and Ringer Cashmere Goat Breeding Farm for high-throughput sequencing of miRNA, lncRNA, mRNA and circRNA. They are all 1.5-year-old females during anagen and in the same growth environment and fed the same feed. Fiber diameter of three adult female LCG skin samples ($d = 19.4 \mu\text{m}$, $19.5 \mu\text{m}$ and $19.8 \mu\text{m}$), there adult female MCG ($d = 13.8 \mu\text{m}$, $14.0 \mu\text{m}$ and $14.1 \mu\text{m}$) 0.1 cm^2 of scapular skin after anesthesia following animal welfare be stored in liquid nitrogen immediately after cleaning until RNA separation. In addition, three coarse and fine skins of Liaoning cashmere goats were collected for high-throughput sequencing of miRNA and qRT-PCR verification. Three LCG (CT-LCG) skin fiber diameter ($d = 19.5 \mu\text{m}$, $19.7 \mu\text{m}$ and $20.2 \mu\text{m}$), three LCG (FT-LCG) skin fiber diameter ($d = 15.3 \mu\text{m}$, $15.4 \mu\text{m}$ and $15.6 \mu\text{m}$).

Experimental procedure. To extract DNA from samples according to Takara kit instructions (Invitrogen, USA). Next, NanoDrop (NanoDrop Technologies, USA) determination RNA purity. Evaluation of RNA integrity using the internationally recognized Agilent 2100 (agilent technologies, USA) and the molar concentration was calculated. Ribosomal RNA consumption is about 5 ug of total RNA. Two sample libraries were constructed with NEBNext (Illumina Corporation, USA) after total RNA extraction. IlluminaHiSeq4000 is finally used for sequencing, and the length of both ends of the sequencing read is $2 \times 150 \text{ bp}$ (pe150).

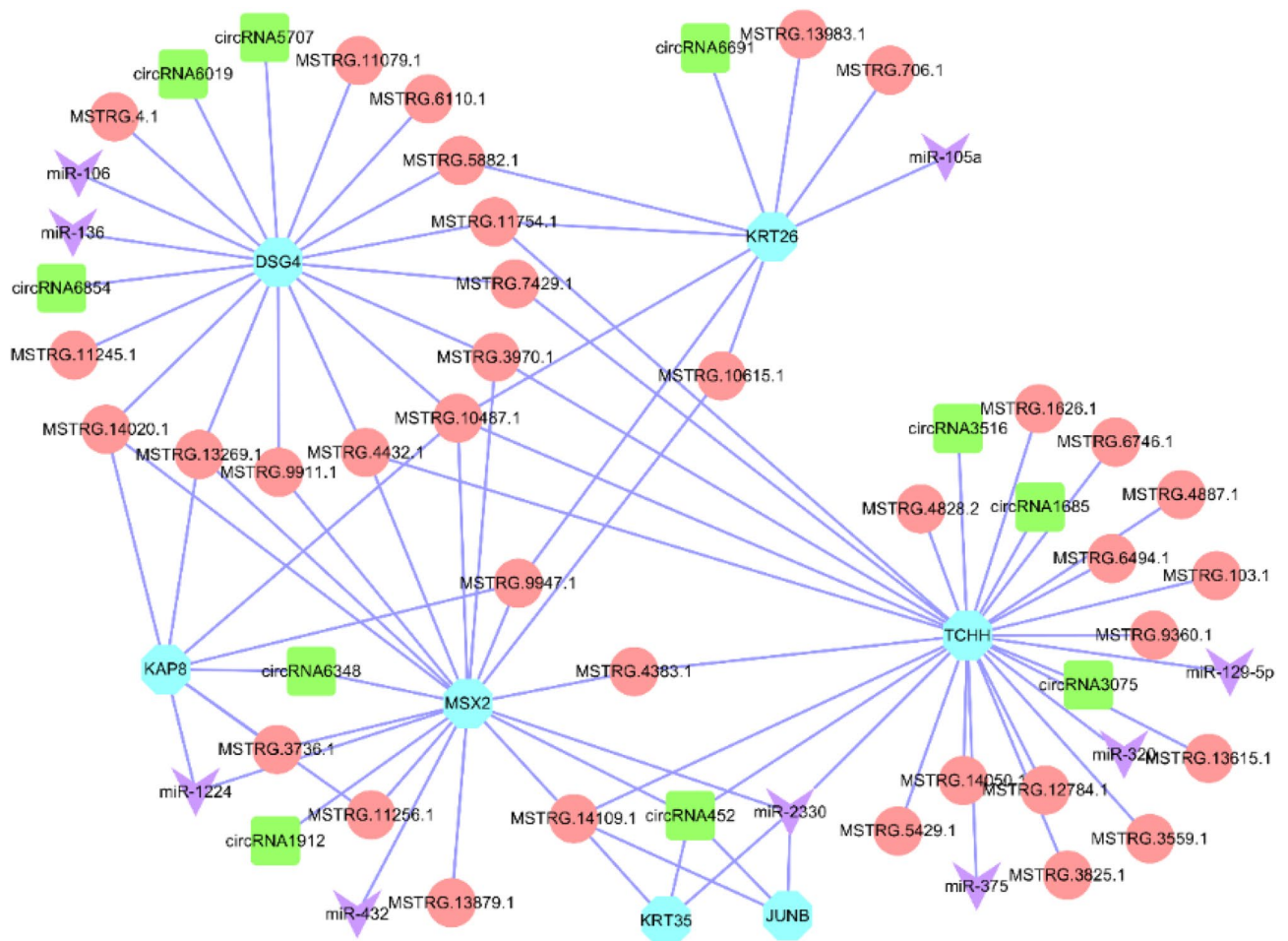


Figure 10. CeRNA networks of 7mRNAs, 35lncRNAs, 10circRNAs and 9miRNAs. Pink: lncRNAs, green: circRNAs, blue: mRNAs, purple: miRNAs.

Bioinformatics process. Firstly, Cutadapt⁵¹ was used to remove the reads that contained adaptor contamination, low quality bases and undetermined bases. Then sequence quality was verified using FastQC (<http://www.bioinformatics.babraham.ac.uk/projects/fastqc/>). We used Bowtie2⁵² and Tophat2⁵³ to map reads to the genome of *Capra hircus*. Remaining reads (unmapped reads) were still mapped to genome using tophat-fusion⁵⁴.

CIRCEplorer^{55,56} was used to de novo assemble the mapped reads to circular RNAs at first; Then, back splicing reads were identified in unmapped reads by tophat-fusion and CIRCEplorer. All samples were generated unique circular RNAs. The differentially expressed circRNAs were selected with \log_2 (fold change) > 1 or \log_2 (fold change) < -1 and with statistical significance (p value < 0.05) by R package—edgeR⁵⁷.

The mapped reads of each sample were assembled using StringTie⁵⁸. Then, all transcriptomes from *Capra hircus* Samples were merged to reconstruct a comprehensive transcriptome using perl scripts. After the final transcriptome was generated, StringTie⁵⁸ and Ballgown⁵⁹ was used to estimate the expression levels of all transcripts.

Differential expression of lncRNAs, circRNAs, mRNAs and miRNAs. Analysis of our sequencing results with data from Liu et al. using R language yielded differentially expressed miRNAs in LCG and MCG. First of all, transcripts that overlapped with known mRNAs and transcripts shorter than 200 bp were discarded. Then we utilized CPC⁶⁰ and CNCI⁶¹ to predict transcripts with coding potential. All transcripts with CPC score < -1 and CNCI score < 0 were removed. The remaining transcripts were considered as lncRNAs. StringTie⁵⁸ was used to perform expression level for mRNAs and lncRNAs by calculating FPKM⁶². The differentially expressed mRNAs and lncRNAs were selected with $|\log_2\text{FoldChange}| \geq 1$ by R package—Ballgown⁵⁹.

Secondly, Cutadapt⁵¹ was used to remove the reads that contained adaptor contamination, low quality bases and undetermined bases. Then sequence quality was verified using by FastQC (<http://www.bioinformatics.babraham.ac.uk/projects/fastqc/>). We used Bowtie2⁵² and Tophat2⁵³ to map reads to the genome of species. Remaining reads (unmapped reads) were still mapped to genome using tophat-fusion⁵⁴. CIRCEplorer^{55,56} was used to de novo assemble the mapped reads to circular RNAs at first; Then, back splicing reads were identified in unmapped reads by tophat-fusion and CIRCEplorer. All samples were generated unique circular RNAs. The differentially expressed circRNAs were selected with \log_2 (fold change) > 1 or \log_2 (fold change) < -1 and with statistical significance (p value < 0.05) by R package—edgeR⁵⁷.

Finally, for the samples with biological replicates: Differential expression analysis of two conditions/groups was performed using the DESeq R package (1.8.3). The p-values was adjusted using the Benjamini and Hochberg method. Corrected p-value of 0.05 was set as the threshold for significantly differential expression by default. For the samples without biological replicates: Differential expression analysis of two samples was performed using the DEGseq (2010) R package. p-value was adjusted using qvalue⁶³. q-value \leq 0.05 and $|\log_2 \text{Fold Change}| \geq 1$ was set as the threshold for significantly differential expression miRNAs by default.

Quantitative real-time PCR. We selected 14 circRNAs, 24 lncRNAs, 24 miRNAs and 7 mRNAs for qRT-PCR verification. Total RNA was isolated from the skin of two groups of samples, each 1 μg of RNA samples were reverse transcribed into cDNA using cDNA, cDNA reverse transcription kit (Takara, Dalian, China). Primer 5.0 was used to design primers for quantitative PCR. Three CT-LCG and three FT-LCG skin samples were subjected to independent experiments and repeated three times each. The *GAPDH* gene was used as an internal control to normalize the expression level of the gene. Graph Pad Prism 5 software was used to display the $2^{-\Delta\Delta\text{CT}}$ method to analyze expressed gene data. Using SPSS for biometric analysis, the difference was considered significant when $p < 0.05$ (* $p < 0.05$; ** $p < 0.001$).

Functional analysis. We predicted target mRNAs based on miRanda's miRNAs, and these target mRNAs are now compared to the differentially expressed mRNAs identified in the RNA-seq results to obtain the intersecting elements of the target mRNA and the differentially expressed mRNAs. DIVAD software was then used to predict the GO function annotation and KEGG⁶⁴ pathway of the intersecting mRNA to analyze its potential function.

ceRNA network construction and bioinformatics analysis. The interactions of lncRNA-miRNA, circRNA-miRNA and mRNA-miRNA were predicted by using TargetScan7.0 and miRanda software. TargetScan 7.0 predicts miRNA targets based on the homology of the seed region⁶⁵, while miRanda is mainly based on the combination of free energy generated by miRNAs in combination with their target genes⁶⁶. The lower the free energy, the stronger the binding. TargetScan has hundreds of quantiles ≥ 50 , and Miranda's maximum free energy value < -10 and Miranda score > 140 are defined as the critical points for target prediction. Based on the data of lncRNA-miRNA, circRNA-miRNA and mRNA-miRNA, Cytoscape 3.6.0 software constructed lncRNA-miRNA-mRNA, circRNA-miRNA-mRNA, lncRNA/circRNA-miRNA-mRNA ceRNA network.

Received: 11 January 2021; Accepted: 25 October 2021

Published online: 09 November 2021

References

- Su, R. *et al.* Transcriptomic analysis reveals critical genes for the hair follicle of Inner Mongolia cashmere goat from catagen to telogen. *PLoS ONE*. <https://doi.org/10.1371/journal.pone.0204404> (2018).
- Berger, J., Buuveibaatar, B. & Mishra, C. The cashmere connection, biodiversity, and climate: Response to von Wehrden *et al.* 2014. *Conserv. Biol.* **29**, 290–292. <https://doi.org/10.1111/cobi.12415> (2015).
- Elton, T. S., Selemón, H., Elton, S. M. & Parinandi, N. L. Regulation of the MIR155 host gene in physiological and pathological processes. *Gene* **532**, 1–12. <https://doi.org/10.1016/j.gene.2012.12.009> (2013).
- Lu, T. X. & Rothenberg, M. E. MicroRNA. *J. Allergy Clin. Immunol.* **141**, 1202–1207. <https://doi.org/10.1016/j.jaci.2017.08.034> (2018).
- Bai, W. L. *et al.* Differential expression of microRNAs and their regulatory networks in skin tissue of liaoning cashmere goat during hair follicle cycles. *Anim. Biotechnol.* **27**, 104–112. <https://doi.org/10.1080/10495398.2015.1105240> (2016).
- Kapranov, P. *et al.* RNA maps reveal new RNA classes and a possible function for pervasive transcription. *Science* **316**, 1484–1488. <https://doi.org/10.1126/science.1138341> (2007).
- Schmitz, S. U., Grote, P. & Herrmann, B. G. Mechanisms of long noncoding RNA function in development and disease. *Cell Mol. Life Sci.* **73**, 2491–2509. <https://doi.org/10.1007/s00018-016-2174-5> (2016).
- Spurlock, C. F. III. *et al.* Expression and functions of long noncoding RNAs during human T helper cell differentiation. *Nat. Commun.* <https://doi.org/10.1038/ncomms7932> (2015).
- Zheng, Y. Y. *et al.* An integrated analysis of cashmere fineness lncRNAs in cashmere goats. *Genes*. <https://doi.org/10.3390/genes10040266> (2019).
- Jin, M. *et al.* Long noncoding RNA and gene expression analysis of melatonin-exposed Liaoning cashmere goat fibroblasts indicating cashmere growth. *Sci. Nat.* <https://doi.org/10.1007/s00114-018-1585-6> (2018).
- Zhang, H.-D., Jiang, L.-H., Sun, D.-W., Hou, J.-C. & Ji, Z.-L. CircRNA: A novel type of biomarker for cancer. *Breast Cancer* **25**, 1–7. <https://doi.org/10.1007/s12282-017-0793-9> (2018).
- Qu, S. *et al.* Circular RNA: A new star of noncoding RNAs. *Cancer Lett.* **365**, 141–148. <https://doi.org/10.1016/j.canlet.2015.06.003> (2015).
- Holdt, L. M., Kohlmaier, A. & Teupser, D. Molecular roles and function of circular RNAs in eukaryotic cells. *Cell. Mol. Life Sci.* **75**, 1071–1098. <https://doi.org/10.1007/s00018-017-2688-5> (2018).
- Zheng, Y. *et al.* Comprehensive analysis of circRNAs from cashmere goat skin by next generation RNA sequencing (RNA-seq). *Sci. Rep.* **10**, 516. <https://doi.org/10.1038/s41598-019-57404-9> (2020).
- Hui, T. Y. *et al.* Discovery and comprehensive analysis of miRNAs from liaoning cashmere goat skin during anagen. *Int. J. Agric. Biol.* **24**, 575–583. <https://doi.org/10.17957/ijab/15.1474> (2020).
- Liu, Z. *et al.* Identification of conserved and novel microRNAs in cashmere goat skin by deep sequencing. *PLoS ONE*. <https://doi.org/10.1371/journal.pone.0050001> (2012).
- Anastasiadou, E., Jacob, L. S. & Slack, F. J. Non-coding RNA networks in cancer. *Nat. Rev. Cancer* **18**, 5–18. <https://doi.org/10.1038/nrc.2017.99> (2018).
- Chan, J. J. & Tay, Y. Noncoding RNA:RNA regulatory networks in cancer. *Int. J. Mol. Sci.* <https://doi.org/10.3390/ijms19051310> (2018).
- Abi, A., Farahani, N., Molavi, G. & Gheibi Hayat, S. M. Circular RNAs: Epigenetic regulators in cancerous and noncancerous skin diseases. *Cancer Gene Ther.* <https://doi.org/10.1038/s41417-019-0130-x> (2019).

20. Zhao, B. *et al.* Systematic analysis of non-coding RNAs involved in the angora rabbit (*Oryctolagus cuniculus*) hair follicle cycle by RNA sequencing. *Front. Genet.* **10**, 407. <https://doi.org/10.3389/fgene.2019.00407> (2019).
21. Wang, Y. *et al.* m6A methylation analysis of differentially expressed genes in skin tissues of coarse and fine type liaoning cashmere goats. *Front. Genet.* <https://doi.org/10.3389/fgene.2019.01318> (2020).
22. Li, Y. *et al.* Comparative proteomic analyses using iTRAQ-labeling provides insights into fiber diversity in sheep and goats. *J. Proteomics* **172**, 82–88. <https://doi.org/10.1016/j.jprot.2017.10.008> (2018).
23. Gao, Y. *et al.* Comparative transcriptome analysis of fetal skin reveals key genes related to hair follicle morphogenesis in cashmere goats. *PLoS ONE* **11**, e0151118. <https://doi.org/10.1371/journal.pone.0151118> (2016).
24. Liu, Y. X. *et al.* Polymorphisms of KAP6, KAP7, and KAP8 genes in four Chinese sheep breeds. *Genet. Mol. Res.* **13**, 3438–3445. <https://doi.org/10.4238/2014.April.30.5> (2014).
25. Kang, X. *et al.* Transcriptome profile at different physiological stages reveals potential mode for curly fleece in Chinese tan sheep. *PLoS ONE* **8**, e71763. <https://doi.org/10.1371/journal.pone.0071763> (2013).
26. Sulayman, A. *et al.* Genome-wide identification and characterization of long non-coding RNAs expressed during sheep fetal and postnatal hair follicle development. *Sci. Rep.* **9**, 8501–8501. <https://doi.org/10.1038/s41598-019-44600-w> (2019).
27. Singh, K. *et al.* JunB defines functional and structural integrity of the epidermo-pilosebaceous unit in the skin. *Nat. Commun.* **9**, 3425–3425. <https://doi.org/10.1038/s41467-018-05726-z> (2018).
28. Florin, L. *et al.* Delayed wound healing and epidermal hyperproliferation in mice lacking JunB in the skin. *J. Investig. Dermatol.* **126**, 902–911. <https://doi.org/10.1038/sj.jid.5700123> (2006).
29. Pisoni, G. *et al.* Differentially expressed genes associated with *Staphylococcus aureus* mastitis in dairy goats. *Vet. Immunol. Immunopathol.* **135**, 208–217. <https://doi.org/10.1016/j.vetimm.2009.11.016> (2010).
30. Su, R. *et al.* Comparative genomic approach reveals novel conserved microRNAs in Inner Mongolia cashmere goat skin and longissimus dorsi. *Mol. Biol. Rep.* **42**, 989–995. <https://doi.org/10.1007/s11033-014-3835-9> (2015).
31. Poller, W. *et al.* Non-coding RNAs in cardiovascular diseases: Diagnostic and therapeutic perspectives. *Eur. Heart J.* **39**, 2704. <https://doi.org/10.1093/eurheartj/ehx165> (2018).
32. Bartel, D. P. MicroRNAs: Target recognition and regulatory functions. *Cell* **136**, 215–233. <https://doi.org/10.1016/j.cell.2009.01.002> (2009).
33. Franco-Zorrilla, J. M. *et al.* Target mimicry provides a new mechanism for regulation of microRNA activity. *Nat. Genet.* **39**, 1033–1037. <https://doi.org/10.1038/ng2079> (2007).
34. Jiao, Q. *et al.* Identification and molecular analysis of a lncRNA-HOTAIR transcript from secondary hair follicle of cashmere goat reveal integrated regulatory network with the expression regulated potentially by its promoter methylation. *Gene* **688**, 182–192. <https://doi.org/10.1016/j.gene.2018.11.084> (2019).
35. Wang, S. *et al.* Integrated analysis of coding genes and non-coding RNAs during hair follicle cycle of cashmere goat (*Capra hircus*). *BMC Genomics* **18**, 767. <https://doi.org/10.1186/s12864-017-4145-0> (2017).
36. Zheng, Y. *et al.* LncRNA-000133 from secondary hair follicle of Cashmere goat: Identification, regulatory network and its effects on inductive property of dermal papilla cells. *Anim. Biotechnol.* **31**, 122–134. <https://doi.org/10.1080/10495398.2018.1553788> (2020).
37. Bai, W. L. *et al.* LncRNAs in secondary hair follicle of cashmere goat: Identification, expression, and their regulatory network in Wnt signaling pathway. *Anim. Biotechnol.* **29**, 199–211. <https://doi.org/10.1080/10495398.2017.1356731> (2018).
38. Li, X., Yang, L. & Chen, L.-L. The biogenesis, functions, and challenges of circular RNAs. *Mol. Cell* **71**, 428–442. <https://doi.org/10.1016/j.molcel.2018.06.034> (2018).
39. Ashwal-Fluss, R. *et al.* circRNA biogenesis competes with pre-mRNA splicing. *Mol. Cell* **56**, 55–66. <https://doi.org/10.1016/j.molcel.2014.08.019> (2014).
40. Hang, D. *et al.* A novel plasma circular RNA circFARSA is a potential biomarker for non-small cell lung cancer. *Cancer Med.* **7**, 2783–2791. <https://doi.org/10.1002/cam4.1514> (2018).
41. Wang, Y., Wang, L., Wang, W. & Guo, X. Overexpression of circular RNA hsa_circ_0001038 promotes cervical cancer cell progression by acting as a ceRNA for miR-337-3p to regulate cyclin-M3 and metastasis-associated in colon cancer 1 expression. *Gene* **733**, 144273. <https://doi.org/10.1016/j.gene.2019.144273> (2020).
42. Chen, G. *et al.* Circular RNA CDR1as promotes adipogenic and suppresses osteogenic differentiation of BMSCs in steroid-induced osteonecrosis of the femoral head. *Bone* <https://doi.org/10.1016/j.bone.2020.115258> (2020).
43. Chen, D. *et al.* The co-expression of circRNA and mRNA in the thymuses of chickens exposed to ammonia. *Ecotoxicol. Environ. Saf.* **176**, 146–152. <https://doi.org/10.1016/j.ecoenv.2019.03.076> (2019).
44. Yin, R. H. *et al.* Discovery and molecular analysis of conserved circRNAs from cashmere goat reveal their integrated regulatory network and potential roles in secondary hair follicle. *Electron. J. Biotechnol.* **41**, 37–47. <https://doi.org/10.1016/j.ejbt.2019.06.004> (2019).
45. Dorn, G. W. II. & Matkovich, S. J. Menage a trois intimate relationship among a microRNA, long noncoding RNA, and mRNA. *Circ. Res.* **114**, 1362–1365. <https://doi.org/10.1161/circresaha.114.303786> (2014).
46. Liu, X. *et al.* Circ-8073 regulates CEP55 by sponging miR-449a to promote caprine endometrial epithelial cells proliferation via the PI3K/AKT/mTOR pathway. *Biochim. Biophys. Acta Mol. Cell Res.* **1865**, 1130. <https://doi.org/10.1016/j.bbamcr.2018.05.011> (2018).
47. Hansen, T. B. *et al.* Natural RNA circles function as efficient microRNA sponges. *Nature* **495**, 384–388. <https://doi.org/10.1038/nature11993> (2013).
48. Zhang, L. *et al.* CircRNA-9119 regulates the expression of prostaglandin-endoperoxide synthase 2 (PTGS2) by sponging miR-26a in the endometrial epithelial cells of dairy goat. *Reprod. Fertil. Dev.* **30**, 1759–1769. <https://doi.org/10.1071/rd18074> (2018).
49. Huang, M. *et al.* Comprehensive analysis of differentially expressed profiles of lncRNAs and circRNAs with associated co-expression and ceRNA networks in bladder carcinoma. *Oncotarget* **7**, 47186–47200. <https://doi.org/10.18632/oncotarget.9706> (2016).
50. Li, X., Ao, J. & Wu, J. Correction: Systematic identification and comparison of expressed profiles of lncRNAs and circRNAs with associated co-expression and ceRNA networks in mouse germline stem cells. *Oncotarget* **9**, 28290. <https://doi.org/10.18632/oncotarget.25674> (2018).
51. Martin, M. CUTADAPT removes adapter sequences from high-throughput sequencing reads. *EMBnet J.* <https://doi.org/10.14806/ej.17.1.200> (2011).
52. Langmead, B. & Salzberg, S. L. Fast gapped-read alignment with Bowtie 2. *Nat. Methods* **9**, 357. <https://doi.org/10.1038/nmeth.1923> (2012).
53. Kim, D. *et al.* TopHat2: Accurate alignment of transcriptomes in the presence of insertions, deletions and gene fusions. *Genome Biol.* <https://doi.org/10.1186/gb-2013-14-4-r36> (2013).
54. Kim, D. & Salzberg, S. L. TopHat-fusion: An algorithm for discovery of novel fusion transcripts. *Genome Biol.* <https://doi.org/10.1186/gb-2011-12-8-r72> (2011).
55. Zhang, X.-O. *et al.* Diverse alternative back-splicing and alternative splicing landscape of circular RNAs. *Genome Res.* **26**, 1277–1287. <https://doi.org/10.1101/gr.202895.115> (2016).
56. Zhang, X.-O. *et al.* Complementary sequence-mediated exon circularization. *Cell* **159**, 134–147. <https://doi.org/10.1016/j.cell.2014.09.001> (2014).

57. Robinson, M. D., McCarthy, D. J. & Smyth, G. K. edgeR: A bioconductor package for differential expression analysis of digital gene expression data. *Bioinformatics* **26**, 139–140. <https://doi.org/10.1093/bioinformatics/btp616> (2010).
58. Pertea, M. *et al.* StringTie enables improved reconstruction of a transcriptome from RNA-seq reads. *Nat. Biotechnol.* **33**, 290. <https://doi.org/10.1038/nbt.3122> (2015).
59. Frazee, A. C. *et al.* Ballgown bridges the gap between transcriptome assembly and expression analysis. *Nat. Biotechnol.* **33**, 243–246. <https://doi.org/10.1038/nbt.3172> (2015).
60. Kong, L. *et al.* CPC: Assess the protein-coding potential of transcripts using sequence features and support vector machine. *Nucleic Acids Res.* **35**, W345–W349. <https://doi.org/10.1093/nar/gkm391> (2007).
61. Sun, L. *et al.* Utilizing sequence intrinsic composition to classify protein-coding and long non-coding transcripts. *Nucleic Acids Res.* <https://doi.org/10.1093/nar/gkt646> (2013).
62. Trapnell, C. *et al.* Transcript assembly and quantification by RNA-Seq reveals unannotated transcripts and isoform switching during cell differentiation. *Nat. Biotechnol.* **28**, 511–U174. <https://doi.org/10.1038/nbt.1621> (2010).
63. Storey, D. J. The positive false discovery rate: A Bayesian interpretation and the q-value. *Ann. Stat.* **31**, 2013–2035 (2003).
64. Kanehisa, M., Sato, Y., Furumichi, M., Morishima, K. & Tanabe, M. New approach for understanding genome variations in KEGG. *Nucleic Acids Res.* **47**, D590–D595. <https://doi.org/10.1093/nar/gky962> (2019).
65. Agarwal, V., Bell, G. W., Nam, J.-W. & Bartel, D. P. Predicting effective microRNA target sites in mammalian mRNAs. *Elife* <https://doi.org/10.7554/eLife.05005> (2015).
66. Betel, D., Wilson, M., Gabow, A., Marks, D. S. & Sander, C. The microRNA.org resource: Targets and expression. *Nucleic Acids Res.* **36**, D149–D153 (2008).

Acknowledgements

Our scientific research was financially aided by four projects: 1. Grants from the National Natural Science Foundation of China (NO. 31802038). 2. The 69th batch of China Postdoctoral Science Foundation (Regional Special Support Program) (NO. 2021M693859). 3. Youth seedling project of Liaoning Provincial Department of Education, China (LSNQN201905). 4. Liaoning Provincial Department of science and technology, agricultural key issues and industrialization project (2020JH2/10200029).

Author contributions

Writing—original draft preparation, T.H.; Methodology, C.Y.; Software, Y.Z.; Validation, T.H., Y.W. and J.S.; Formal analysis, Z.B.; Investigation, X.Z.; Language editing and modification, W.C.; Data curation, T.H.; Writing—review and editing, Z.W. and W.B.; Funding acquisition, Z.W. and W.B.

Competing interests

The authors declare no competing interests.

Additional information

Correspondence and requests for materials should be addressed to Z.W.

Reprints and permissions information is available at www.nature.com/reprints.

Publisher's note Springer Nature remains neutral with regard to jurisdictional claims in published maps and institutional affiliations.



Open Access This article is licensed under a Creative Commons Attribution 4.0 International License, which permits use, sharing, adaptation, distribution and reproduction in any medium or format, as long as you give appropriate credit to the original author(s) and the source, provide a link to the Creative Commons licence, and indicate if changes were made. The images or other third party material in this article are included in the article's Creative Commons licence, unless indicated otherwise in a credit line to the material. If material is not included in the article's Creative Commons licence and your intended use is not permitted by statutory regulation or exceeds the permitted use, you will need to obtain permission directly from the copyright holder. To view a copy of this licence, visit <http://creativecommons.org/licenses/by/4.0/>.

© The Author(s) 2021